THE POROSITY, PERMEABILITY AND RESTRUCTURING OF HETEROGENEOUS FILTER CAKES

Kuhan Chellappah[1,2], Steve Tarleton[1] (e.s.tarleton@lboro.ac.uk) and Richard Wakeman[3]
[1]Dept Chemical Engineering, Loughborough University, Loughborough, Leics., LE11 3TU, UK.
[2]BHR Group Ltd, Cranfield, Bedfordshire, MK43 0AJ, UK.
[3]Consultant Chemical Engineer, Exeter, EX5 1DD, UK.

ABSTRACT

The constant pressure filtration characteristics of cellulose fibres, titania (rutile) and mixtures of the two were studied using an automated filtration apparatus. With filtrations at 450 kPa, the average permeability (k_{av}) for pure fibre and rutile were approximately 3.2×10^{-17} and 1.3×10^{-16} m^2 respectively, with the variation of k_{av} with fibre fraction showing a maximum. Similar trends were observed at filtration pressures of 150 and 600 kPa. The porosities (ε_{av}) of filter cakes formed from pure fibre and rutile suspensions were approximately 0.75 and 0.6 respectively. Interparticle penetration and additive porosity models were applied to the porosity data, and the additive porosity model appeared to better represent the experimental data. Also, the results obtained suggest that abrupt transitions in cake structure occur part way through some filtrations, resulting in anomalous filtration behaviour.

KEYWORDS

Filtration; Sedimentation; Binary suspensions; Agglomeration; Permeability; Porosity.

INTRODUCTION

The packing behaviour of constituent solids influences the properties of a filter cake to a large extent. Typical theoretical predictions for spherical binary mixtures almost always show a maximum packing at some intermediate mixture fraction (generally attributed to interparticle penetration) [1-3]; these works have mainly studied the packing of binary mixtures but not in terms of filtration behaviour and hence did not pay attention to the permeability of the packed beds. Some other works [4-7] have studied more specifically the filtration behaviour of binary mixtures, but these works have generally only considered mixtures of two particle species. However, with many industries such as nuclear waste treatment, water and wastewater treatment, and paper and pulp, the heterogeneous suspensions to be dewatered are often complex mixtures of fibres, fibre fines, and several particle species. More recently, some work [8,9] has focused on the filtration of heterogeneous fibre/particle mixtures. In these works, initial results from cellulose fibre/titania (rutile) suspension filtration and sedimentation experiments were presented.

Various works [10-15] have previously reported abrupt changes in cake structure part way through a filtration leading to unexpected filtrate flow behaviour, and have attributed them to various potential causes. When such anomalous filtration behaviour is not well understood, this could lead to erroneous scale up and cycle time calculations. Rietema [10] noted transitions in cake structure leading to unexpected reductions in filtrate flow rate during the filtration of polyvinyl chloride particles in water and claimed that the most likely explanation was destabilization of the cake structure. The higher filtrate flow through the cake toward the start of filtration was deemed to stabilize it prior to a flow transition point at which so called 'retarded packing compressibility' (RPC) occurred. Other explanations for this sudden anomalous filtration behaviour include the formation of unobstructed channels within the cake [14], and a migration of fines/compression mechanism [13]. Tarleton and Morgan [15] assess the likelihood of the various mechanisms and point out that

Cite paper as: Chellappah K., Tarleton E.S. and Wakeman R.J., 2010, The porosity, permeability and restructuring of heterogeneous filter cakes, *Chemical Engineering & Technology*, **33**, 1-8. DOI: 10.1002/ceat.201000093

an abrupt change in cake form is more likely during the filtration of suspensions containing loosely networked particles.

This paper discusses the porosity and permeability trends with cellulose fibre/titania (rutile) filter cakes. Suspension settling data is presented to help interpret the filtration data. Some filtration results which show unexpected filter cake restructuring are also presented and discussed.

EXPERIMENTAL

Apparatus and Methods

A computer controlled, laboratory scale, pressure filtration apparatus capable of automated data acquisition was used for the filtration experiments. The hardware comprised a stainless steel (s/s) deadend Nutsche filter of 120 cm^2 area and a s/s suspension storage vessel connected by s/s piping and computer controlled electro-pneumatic valving. The filtration pressure was maintained at a constant level via an electronically driven regulator whilst filtrate flow was determined via successive readings from an electronic balance. Further details of the apparatus can be found elsewhere [16,17]. The filter medium was a Gelman Versapor 0.2 μm rated membrane. A new membrane was used in each experiment and this yielded a visually clear filtrate in all cases. Sedimentation experiments were carried out in a plastic graduated cylinder of 360 mm length and 60 mm inner diameter. The suspension-supernatant interface height and corresponding elapsed time were recorded at suitable intervals.

Suspensions comprising either pure fibres, or rutile, or binary mixtures of the two, in deionized water (DI), were used in experiments. Total solids concentration was maintained at 1.1% v/v. In an experiment involving a binary mixture, rutile was added into the suspending medium and mixed for 30 minutes at 600 rpm prior to fibre addition in order to reduce problems relating to dispersion. The final suspension was stirred for ~3 h at 800 rpm with a flat blade stirrer prior to a filtration or sedimentation experiment. Care was taken to ensure that suspensions were well mixed to minimize batch to batch variations. Experiments were carried out at a constant temperature of 21±2ºC and over a narrow pH range. The pH of suspensions in DI water varied from ~8.4 (pure rutile) to ~7.6 (pure fibres).

Materials and Characterisation

The fibres used were in the form of tissue paper (Merton Cleaning Supplies (Leicester) Ltd). When the tissue paper was dispersed into DI water two types of suspended solids were produced, cellulose fibres and the fillers associated with the tissue. Energy dispersive X-ray spectroscopy (EDX) determined calcite to be the filler and acid washing coupled with a mass balance determined that ~4.8% by volume of the tissue paper consisted of these calcite fillers. The titania was in the form of the rutile polymorph and obtained from Huntsman. Rutile particle size distributions and zeta (ζ) potentials in DI water were measured using a Malvern Zetasizer 3000 HS. The size (width) distributions of the fibres were obtained by measuring more than a hundred fibres at various magnifications of SEM image. Solids shapes and aspect ratios were estimated from SEM images. Further characterisation of the solids, and relevant SEM images have been given in a previous paper [8]. Some relevant properties of the fibres and rutile are summarized in Table 1.

RESULTS AND DISCUSSION

The experimental data presented are representative of the dataset obtained in this study. The effects of solids composition is expressed in terms of the variable X_D which is defined as the ratio of the volume of fibres to the total volume of solids in the suspension; $X_D = 0$ indicates a pure rutile suspension (i.e. no fibres) whereas $X_D = 1$ indicates a pure fibre suspension (i.e. no rutile).

Cite paper as: Chellappah K., Tarleton E.S. and Wakeman R.J., 2010, The porosity, permeability and restructuring of heterogeneous filter cakes, *Chemical Engineering & Technology*, **33**, 1-8. DOI: 10.1002/ceat.201000093

Two important parameters in the analysis of cake filtration are the filter cake average porosity (ε_{av}) and permeability (k_{av}). The cake average permeability embraces the cake properties affecting the nature of fluid flow through the voids, and is related to the filter cake average specific resistance (α_{av}) by:

$$k_{av} = \frac{1}{\rho_s (1-\varepsilon_{av}) \alpha_{av}} \quad (1)$$

The cake average porosity was calculated using:

$$\varepsilon_{av} = 1 - \frac{w}{\frac{Vs}{A}\left(\frac{\rho_s (m-1) + \rho_l}{1-ms}\right)} \quad (2)$$

where V is the filtrate volume, A the filtration area, ρ_l the liquid density, ρ_s the solids density, s the solids mass fraction in the feed, w the mass of dry solids deposited per unit filtration area, and m the ratio of mass of wet cake to the mass of dry cake as measured at the end of filtration. The cake specific resistance was determined in the conventional manner from the linear portion of dt/dV vs. V filtration plots, from the following equation:

$$\frac{dt}{dV} = \frac{\mu \alpha_{av} \rho_l s}{A^2 \Delta P (1-ms)} V + \frac{\mu R_m}{A \Delta P} \quad (3)$$

Sedimentation results are presented in the form of initial settling rates and proportion of sludge vs. X_D. Initial settling rate in a sedimentation test was determined from a graph of suspension-supernatant interface height vs. time, where the initial points fall on a straight line whose gradient can be calculated. The proportion of sludge is the final sediment height (after 24 h settling) expressed as a percentage of the initial suspension height.

General Sedimentation and Filtration Behaviour

Figure 1 shows batch sedimentation results for suspensions of various solids compositions in deionized water. It appears that pure rutile and pure fibre form stable suspensions which do not readily settle. With only small amounts of fibres added to a pure rutile suspension, rutile-fibre interactions take place and the suspension destabilizes. The initial settling rate continues to increase with X_D up to the point where ~50% by volume of the solids consists of rutile, presumably due to the increasing surface area available for interaction. Further increases in X_D caused a sharp reduction in initial settling rate until approximately 75% v/v of the solids consisted of fibres, and subsequent increases in X_D rendered the suspension essentially stable once again. Also, it is not surprising that the proportion of sludge data suggests that fibres form more loosely networked packings than rutile.

An example dt/dV vs. V plot for a 450 kPa filtration of an X_D = 0.928 suspension in deionized water is shown in Figure 2. An interesting observation in the present study was the presence of abrupt changes in the filtrate flow rate part way through some filtrations. For example, Figure 2 suggests that some unexpected and sudden restructuring of the filter cake resulted in an increased filtration rate. Such transitions in cake structure have been noted sporadically by previous workers (summarized by Tarleton and Morgan [15]) and attributed to the migration of fines, cake collapse and/or formation of channels within the cake. These abrupt transitions are discussed further in a latter part of this paper.

Cite paper as: Chellappah K., Tarleton E.S. and Wakeman R.J., 2010, The porosity, permeability and restructuring of heterogeneous filter cakes, *Chemical Engineering & Technology*, **33**, 1-8. DOI: 10.1002/ceat.201000093

Figures 3 and 4 illustrate the effects of solids composition and filtration pressure on ε_{av} and k_{av}, respectively. It is seen that the average cake porosity appears to progressively increase from pure rutile cakes to pure fibre cakes. The average cake permeability experienced a maxima at $0.4 < X_D < 0.8$. It is seen that compared to the influence of solids composition, the influence of filtration pressure on the filter cake average porosity and permeability was less significant. The behaviour shown in Figures 3 and 4 are further interpreted in the following sections.

Filter Cake Porosity

Typical theoretical predictions for spherical binary mixtures show a minimum in the variation of porosity with solids composition, and a larger difference in size between the coarse and fine solids generally yields a more pronounced non-linearity [1-3]. However, in this study, the variation of porosity with volume fraction of fibres is shown to be relatively limited and in many cases almost linear despite the fibres being of wide size distribution and generally several orders of magnitude larger than the rutile particles. By way of example, two models are presented and compared to illustrate the fibre/rutile packing characteristics. These two models are taken to be representative of two approaches; the first attempts to describe the concept of interparticle penetration [3], and the second the concept of additive porosity [4].

After presenting a system of equations, Dias and co-workers [3] reduced them to two equations, one for a packed bed rich in small particles:

$$\varepsilon_{av} = \varepsilon_{av,2}\left(\frac{1-X_D}{1-\varepsilon_{av,2}X_D}\right) \tag{4}$$

and another for a packed bed rich in large particles:

$$\varepsilon_{av} = 1-\frac{1-\varepsilon_{av,1}}{X_D} \tag{5}$$

where $\varepsilon_{av,1}$ is the average porosity of a bed of large particles (fibres in this case) and $\varepsilon_{av,2}$ the average porosity of a bed of small particles (rutile in this case). Plots of equation (4) and (5) vs. solids composition, with equation (4) emanating from the pure small component and equation (5) emanating from the pure large component, will result in two curves which intersect at some intermediate solids composition. This point of intersection is generally taken to be representative of a minimum porosity and indicates a transition from one dominant mechanism to another. Discontinuation of these two curves beyond the intersection point results in one smooth curve which attempts to describe the variation of porosity with solids composition. Equations (4) and (5) correspond to the classic linear mixing model, which has been developed in some previous works [3,18,19]. Using the additive porosity model [4] on the other hand, the additive porosity is given by the sum of the void volumes divided by the sum of the total volumes due to each component:

$$\varepsilon_{av} = \frac{\frac{\varepsilon_{av,1}X_D}{1-\varepsilon_{av,1}} + \frac{\varepsilon_{av,2}\left(1-X_D\right)}{1-\varepsilon_{av,2}}}{\frac{X_D}{1-\varepsilon_{av,1}} + \frac{1-X_D}{1-\varepsilon_{av,2}}} \tag{6}$$

Predictions of ε_{av} given by equations (4) and (5) for cakes formed at 450 kPa were plotted in Figure 5 along with the experimental data. Predictions given by the additive porosity model (equation (6)) are also included in this figure. It is seen that the concept of additive porosity is apparently more representative of the experimental data than the interparticle penetration model used (equations (4) and (5)). Assuming the theoretical justifications of both models hold, this brings about some physical implications. With the additive law, the filling of a pore volume generated by one

Cite paper as: Chellappah K., Tarleton E.S. and Wakeman R.J., 2010, The porosity, permeability and restructuring of heterogeneous filter cakes, *Chemical Engineering & Technology*, **33**, 1-8. DOI: 10.1002/ceat.201000093

component by another (finer) component cannot be described. On the other hand, the interparticle penetration model takes this filling of pore volume into account. Since the additive model fits better, the fibres may be coated by rutile to reduce the interfibre porosity to a small extent, instead of the rutile freely migrating within the fibre network (which would have led to a minimum porosity at some intermediate solids composition). Since a pure rutile packing gives a lower porosity than a pure fibre packing, this explains why the porosity generally decreases with increasing rutile content. Figure 5 may suggest that the general concept of additive porosity seems to be better than interparticle penetrations when one particle is adsorbed onto the surfaces of the other.

Filter Cake Permeability

The trend of k_{av} with solids composition passes through a maximum in the region $0.4 < X_D < 0.8$ (see Figure 4). This is an interesting result as in many cases specific resistance has previously been reported to decrease gradually and become lowest when $X_D = 1$ [4,6]. However, a minimum in α_{av} (suggesting a maximum in average permeability) at an intermediate X_D value was more recently reported [7] when aggregation occurred between the two solids (rutile and silica) being filtered from the binary mixture. Iritani *et al*. [7] did not observe a minimum in α_{av} in the absence of such aggregation. Similarly, the reason for the convex k_{av} vs. X_D trend observed in the present work is rutile-fibre aggregation.

The k_{av} vs. X_D trend generally corresponds to the trend of initial settling rate vs. X_D (see Figure 1); this is not surprising as the initial settling rates were largely influenced by the degree of aggregation. It is well known in flocculation/coagulation studies that a maximum permeability can coincide with a maximum settling rate. Further, the influence of simultaneous sedimentation with filtration is most significant for suspensions which give the greatest initial settling rates. However, a more explicit relationship between k_{av} and initial settling rate cannot be easily formulated.

An increase in fibre volume fraction (X_D) results in somewhat more porous cakes (larger ε_{av}) and also in a greater mean 'size'. Hence, increasing values of X_D may be expected to result in more permeable filter cakes. However, it should be noted that the solids form changes with fibre fraction. The fibres and rutile are of very different forms, with the rutile being more isometric in shape, and this is likely to result in varying packing mechanisms moving from pure rutile to pure fibre cakes. Also, possible fibre-rutile interactions will further influence the specific surface exposed to fluid flow at the various solids compositions, which in turn will affect the specific resistance. In addition, when fibres dominate the filtration further complexity is introduced by a fibre's ability to coil up and 'mat out' [8]. Yet more complications arise due to the presence of solids of widely varying shapes and sizes in the fibrous suspension with fines potentially present under conditions conducive to blinding of the forming cake. Supporting evidence for the presence of fines is the fact that filtrations of fibre suspensions proceeded at an extremely slow rate using a 4 µm rated filter cloth and the turbid supernatant of a settled fibrous suspension.

Filter Cake Restructuring

With some filtrations, restructuring of the filter cake occurred part way through the filtration resulting in deviations from expected filtration behaviour and this was generally reproducible. This phenomenon was not noted with rutile rich cakes, presumably because the rutile particles were more discrete and closely packed. The occurrence of abrupt changes to cake structure part way through the filtration of a fibre suspension was limited to higher filtration pressures (above ~400 kPa); there was no evidence of RPC or related phenomena during experiments performed at filtration pressures of 300 kPa and below. In Figure 6, a phenomenon showing a significant deviation from the 'expected' filtration behaviour (i.e. linear plot of reciprocal filtration rate vs. cumulative filtrate volume) was apparent for the filtration of pure fibre suspensions at a filtration pressure of 450 kPa but not for filtration pressures of 150 and 300 kPa. After approximately 3×10^{-4} m^3 of filtrate had been produced, the cakes formed during the 150 and 300 kPa filtrations undergo cake deliquoring (at approximately point A in Figure 6). On the other hand, the cake formed during

Cite paper as: Chellappah K., Tarleton E.S. and Wakeman R.J., 2010, The porosity, permeability and restructuring of heterogeneous filter cakes, *Chemical Engineering & Technology*, **33**, 1-8. DOI: 10.1002/ceat.201000093

the 450 kPa filtration underwent an abrupt transition in structure, evidenced by the marked change increase in filtrate flow rate.

Figure 7 illustrates the effects of cake restructuring on the instantaneous filtrate flow rate for filtrations of pure fibre suspensions at filtration pressures of 450, 550 and 600 kPa. In all cases the changes in cake structure were accompanied by approximately an order of magnitude increase in filtrate flow rate. The filtrate flow rate just before the abrupt transition in cake structure is denoted $(dV/dt)|_{tr}$ and changes to the cake structure increased the filtrate flow rate from $(dV/dt)|_{tr}$ to a maximum peak of $(dV/dt)|_{tr,max}$. At 450 kPa this change was from approximately $1x10^{-7}$ m^3 s^{-1} to $1.3x10^{-6}$ m^3 s^{-1}, at 550 kPa from approximately $1.1x10^{-7}$ m^3 s^{-1} to $1.5x10^{-6}$ m^3 s^{-1}, and at 600 kPa from approximately $2.6x10^{-7}$ m^3 s^{-1} to $1.9x10^{-6}$ m^3 s^{-1}. Generally, when restructuring of the filter cake led to increases in the filtrate flow rate, the maximum peak reached increased with filtration pressure. The effects of simultaneous sedimentation are ruled out as a possible cause of the observed filtration behaviour as sedimentation effects cannot increase the flow rate, as seen in this work.

Figure 8 illustrates the effects of solids composition on cake restructuring and suggests that the addition of rutile resulted in marginally less pronounced deviations from the 'expected' filtration behaviour. This effect of rutile addition is seen by comparing the difference between the inverse of the filtrate flow rates just before the transition with the corresponding inverse of the maximum filtrate flow rates during the transition, for the three different solids compositions. Addition of more significant amounts of rutile past a critical concentration altered the nature and hence outcomes of cake restructuring altogether, as illustrated by Figure 9. By way of example, unlike with suspensions of $X_D \geq 0.928$, filtration plots for $X_D = 0.859$ and $X_D = 0.764$ exhibit a pronounced increase in filtration resistance (upward curvature of the dataset) prior to a relatively short period of increased filtration rate. To further illustrate this, with $X_D = 0.859$, it can be seen from Figure 9 that the upward curvature starts at point A. This increase in filtration resistance (reduction in filtration rate) at point A can be seen more clearly in Figure 10 which shows the filtrate flow rate profile corresponding to the reciprocal flow rate on Figure 9 at $X_D = 0.859$. The regression curve in Figure 10 was obtained based on the experimental data points before point A. It is seen that the relatively short period of increased filtration rate takes place from ~150 s to point B, and is small in magnitude when compared to, for instance, the suspensions with less rutile in Figure 8.

Previous works [10-15] which have reported broadly similar phenomena have generally observed the consequences sporadically (without much control over when it occurs) and exclusively reported either a resultant increase or decrease in filtration rate. It is, perhaps interestingly, seen in this work that not only were the changes in cake structure relatively reproducible, but also the nature of the change can be altered by changes in filtration pressure and solids composition. Further investigations into the underlying mechanisms involved are currently being carried out.

CONCLUSIONS

Porosity and permeability trends with solids composition for the filtration of fibre/rutile mixtures corresponded with the sedimentation data. Physico-chemical interactions were suggested to be the most likely cause of maxima in the trends of initial settling rate and filter cake average permeability with solids composition. The general concept of additive porosity seems to be better than interparticle penetration when one particle is adsorbed onto the surfaces of the other. Interesting and reproducible transitions in filter cake structure part way through some filtrations have been presented and discussed.

NOMENCLATURE

A filtration area (m^2)

Cite paper as: Chellappah K., Tarleton E.S. and Wakeman R.J., 2010, The porosity, permeability and restructuring of heterogeneous filter cakes, *Chemical Engineering & Technology*, **33**, 1-8. DOI: 10.1002/ceat.201000093

k_{av} average filter cake permeability (m^2)
m ratio of mass of wet cake to mass of dry cake (-)
ΔP filtration pressure (Pa)
R_m filter medium resistance (m^{-1})
s mass fraction of solids in suspension (-)
t cake formation time (s)
V cumulative filtrate volume (m^3)
w mass of dry solids deposited per unit area (kg m^{-2})
X_D ratio of volume of fibres to total volume of solids in the binary suspensions (-)

α_{av} average specific resistance of a filter cake (m kg^{-1})
ε_{av} average filter cake porosity (-)
ρ_l liquid density (kg m^{-3})
ρ_s solids true density, effective solids density for binary mixtures (kg m^{-3})

REFERENCES

1. B. Yu and N. Standish, *Powder Technol.*, 1988, **55**(3), 171.

2. M. Mota, J.A. Teixeira, W.R. Bowen and A. Yelshin, *Filtration*, 2001, **1**(4), 101.

3. R. Dias, J.A. Teixeira, M. Mota and A. Yelshin, *Ind. Eng. Chem. Res.*, 2004, **43**(24), 7912.

4. M. Shirato, M. Sambuichi and S. Okamura, *AIChE J.*, 1963, **9**(5), 599.

5. E. Abe and H. Hirosue, *J. Chem. Eng. Jpn.*, 1982, **15**(6), 490.

6. R.J. Wakeman, *Proc. 7th World Filtr. Congr.*, 1, pp.234-238, Budapest, 1996.

7. E. Iritani E., Y. Mukai and Y. Toyoda, *J. Chem. Eng. Jpn.*, 2002, **35**(3), 226.

8. K. Chellappah, E.S. Tarleton and R.J. Wakeman, *Filtration*, 2009, **9**(4), 286.

9. K. Chellappah, E.S. Tarleton and R.J. Wakeman, *Proc. Filtech Conf.*, *1*, pp.260-267, Wiesbaden, 2009.

10. K. Rietema, *Chem. Eng. Sci.*, 1953, **2**(2), 88.

11. R.L. Baird and M.G. Perry, *Filtr. Sep.*, 1967, **4**, 47.

12. P.B. Sørensen, *PhD. Thesis*, Aalborg University, Aalborg, 1992.

13. P.B. Sørensen, J.R. Christensen and J.H. Bruus, *Water Environ. Res.*, 1995, **67**(1), 25.

14. M. Fathi-Najafi and H. Theliander, *Sep. Technol.*, 1995, **5**(3), 165.

15. E.S. Tarleton and S.A. Morgan, *Filtration*, 2001, **1**(4), 93.

16. E.S. Tarleton and R.C. Hadley, *Filtration*, 2003, **3**(1), 40.

17. E.S. Tarleton, *J. Chin. Inst. Chem. Eng.*, 2008, **39**(2), 151.

18. B. Yu and N. Standish, *Ind. Eng. Chem. Res.*, 1991, **30**(6), 1372.

Cite paper as: Chellappah K., Tarleton E.S. and Wakeman R.J., 2010, The porosity, permeability and restructuring of heterogeneous filter cakes, *Chemical Engineering & Technology*, **33**, 1-8. DOI: 10.1002/ceat.201000093

19. B. Yu, R.P. Zou and N. Standish, *Ind. Eng. Chem. Res.*, 1996, **35**(10), 3730.

Cite paper as: Chellappah K., Tarleton E.S. and Wakeman R.J., 2010, The porosity, permeability and restructuring of heterogeneous filter cakes, *Chemical Engineering & Technology*, **33**, 1-8. DOI: 10.1002/ceat.201000093

FIGURES AND TABLES

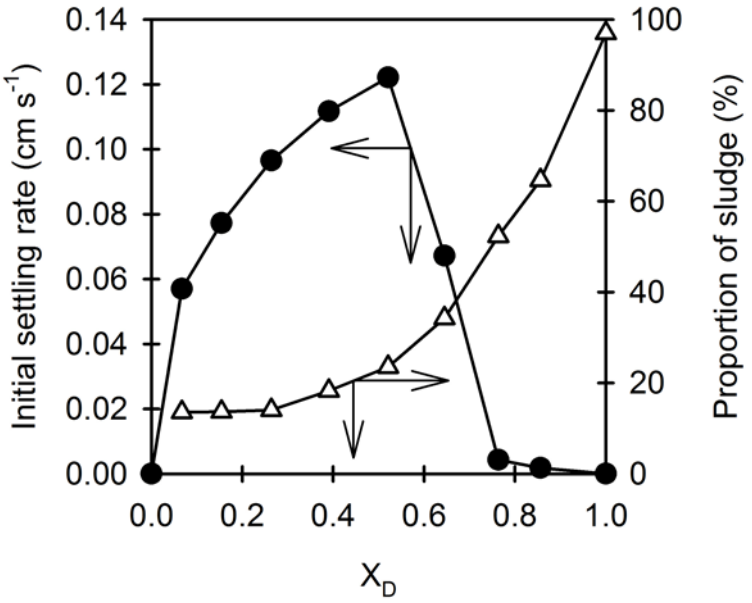

Figure 1: Effect of fibre fraction (X_D) on the initial settling rate and proportion of sludge.

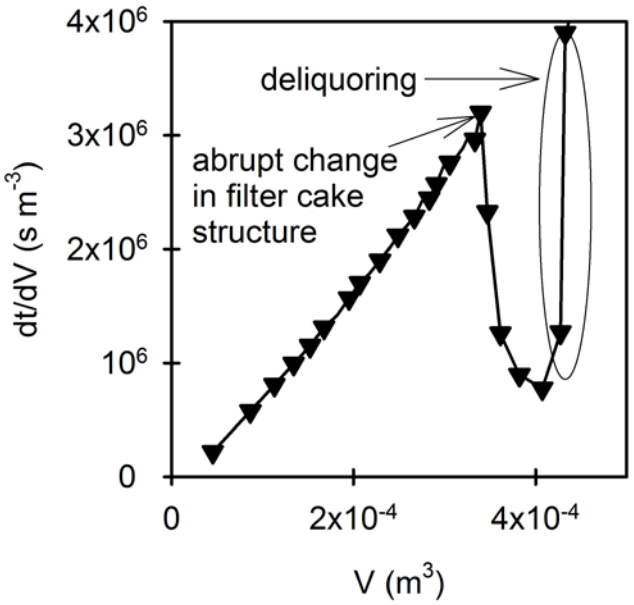

Figure 2: Example filtration plot for the 450 kPa filtration of an X_D = 0.928 suspension. The point where cake restructuring first occurs is shown.

Cite paper as: Chellappah K., Tarleton E.S. and Wakeman R.J., 2010, The porosity, permeability and restructuring of heterogeneous filter cakes, *Chemical Engineering & Technology*, **33**, 1-8. DOI: 10.1002/ceat.201000093

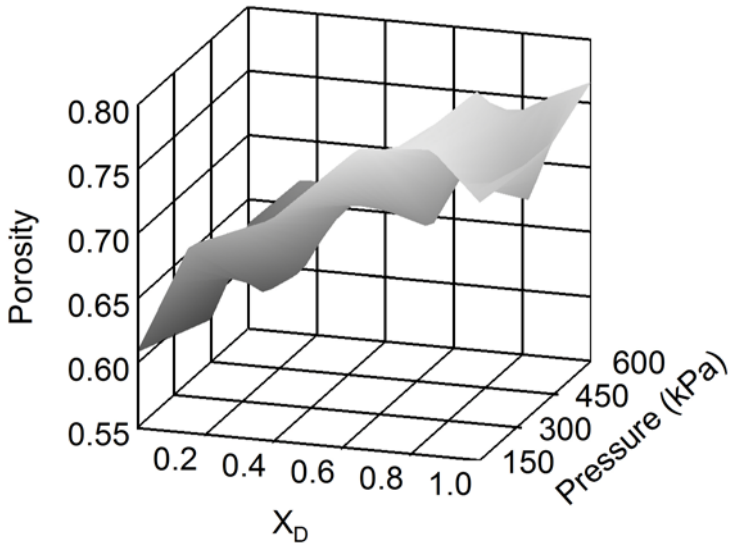

Figure 3: Effects of solids composition and filtration pressure on filter cake average porosity.

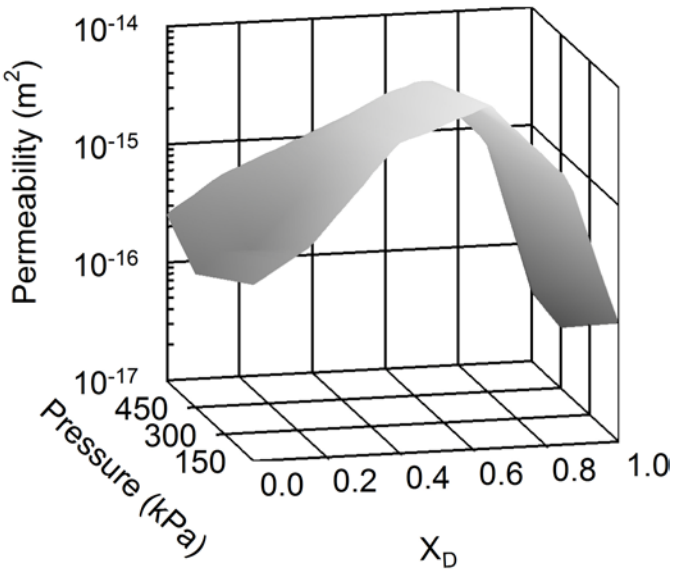

Figure 4: Effects of solids composition and filtration pressure on filter cake average permeability.

Cite paper as: Chellappah K., Tarleton E.S. and Wakeman R.J., 2010, The porosity, permeability and restructuring of heterogeneous filter cakes, *Chemical Engineering & Technology*, **33**, 1-8. DOI: 10.1002/ceat.201000093

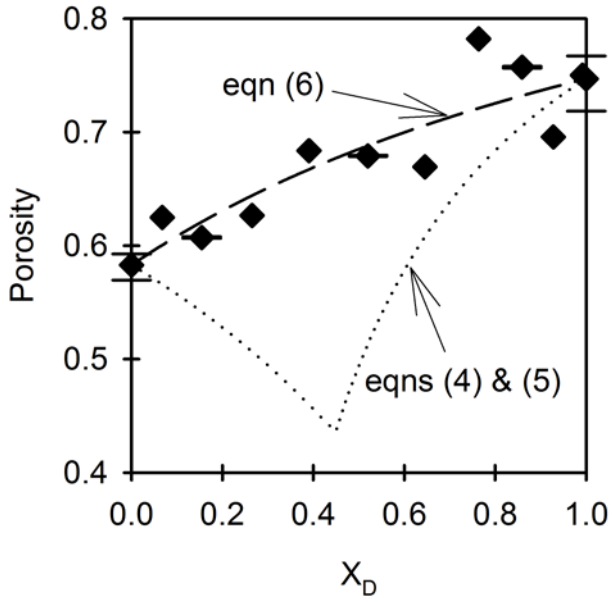

Figure 5: Predictions given by equations (4) and (5) (interparticle penetration model) and equation (6) (additive model) are plotted along with the experimental porosity data for 450 kPa filtrations.

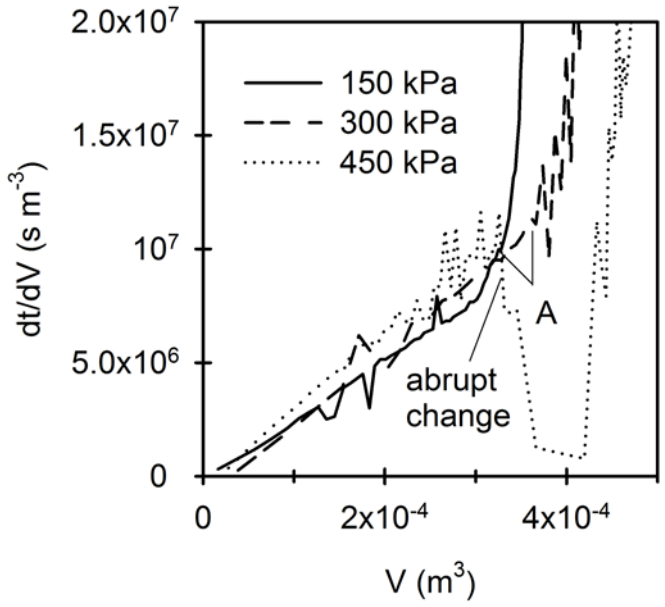

Figure 6: Filtration plots for fibre suspensions at three filtration pressures. Cake deliquoring begins at point A except at 450 kPa, where an abrupt restructuring of the filter cake occurred before deliquoring.

Cite paper as: Chellappah K., Tarleton E.S. and Wakeman R.J., 2010, The porosity, permeability and restructuring of heterogeneous filter cakes, *Chemical Engineering & Technology*, **33**, 1-8. DOI: 10.1002/ceat.201000093

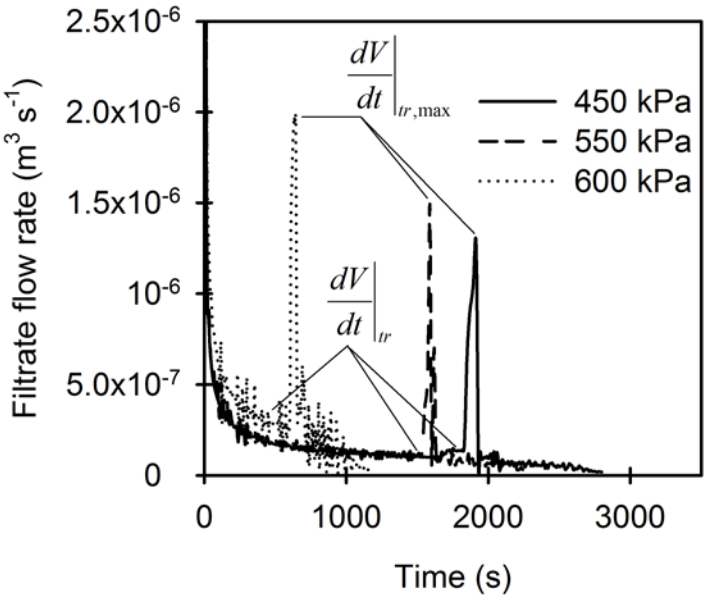

Figure 7: Filtrate flow rate profile for pure fibre suspensions at three filtration pressures.

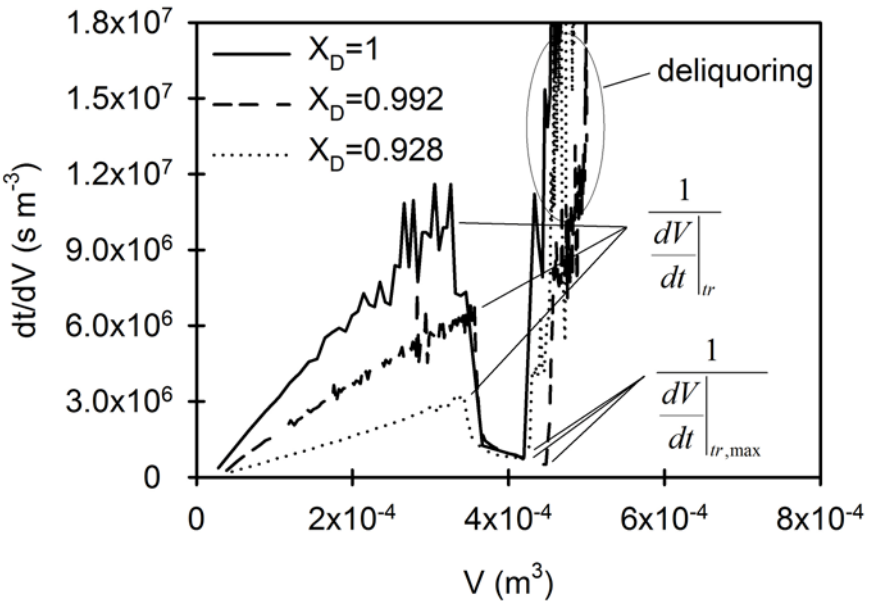

Figure 8: Filtration plots for binary suspensions of various solids compositions (fibre rich suspensions) at 450 kPa.

Cite paper as: Chellappah K., Tarleton E.S. and Wakeman R.J., 2010, The porosity, permeability and restructuring of heterogeneous filter cakes, *Chemical Engineering & Technology*, **33**, 1-8. DOI: 10.1002/ceat.201000093

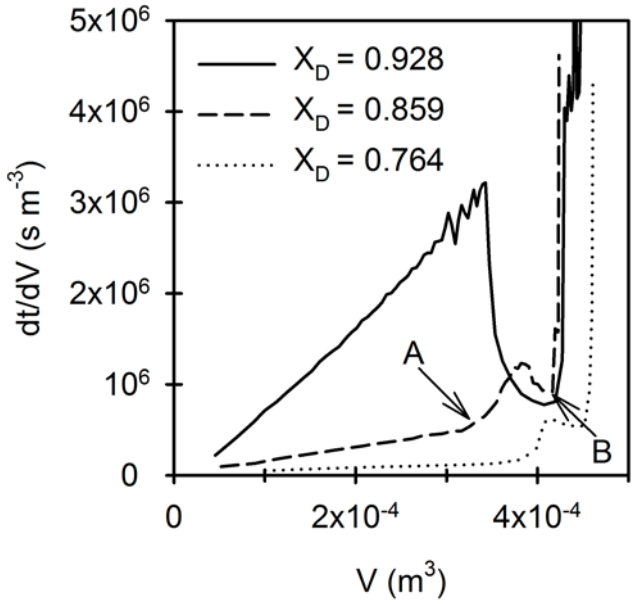

Figure 9: Filtration plots for binary suspensions of various solids compositions (from fibre rich to intermediate solids compositions) at 450 kPa.

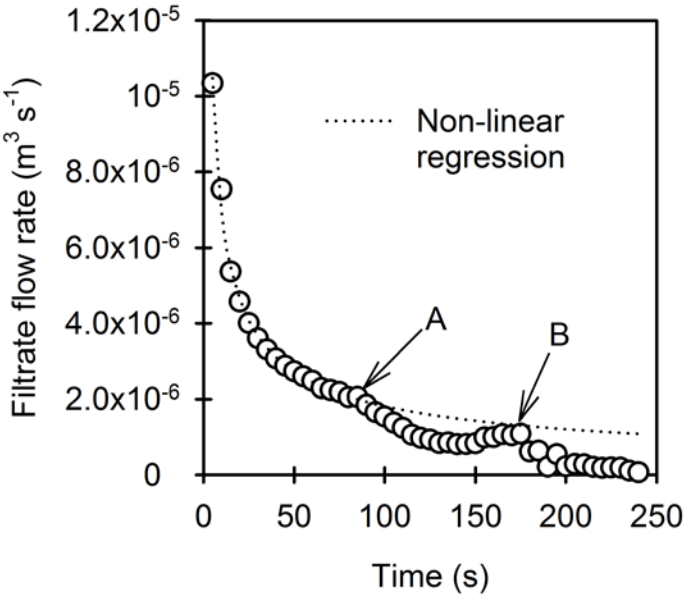

Figure 10: Filtrate flow rate profile for an X_D = 0.859 suspension. The data, and points A and B, correspond with those in Figure 9 at X_D = 0.859.

Cite paper as: Chellappah K., Tarleton E.S. and Wakeman R.J., 2010, The porosity, permeability and restructuring of heterogeneous filter cakes, *Chemical Engineering & Technology*, **33**, 1-8. DOI: 10.1002/ceat.201000093

	10% size (µm)	50% size (µm)	90% size (µm)	Shape	Aspect ratio	ζ-potential in DI water (mV)
Rutile	0.4	0.45	0.7	Elliptical	2-4	-35
Fibres	6[(a)]	15[(a)]	29[(a)]	non-cylindrical, angular	~100	-18

[(a)] Width for fibres

Table 1: Relevant properties of the two solids used.

Cite paper as: Chellappah K., Tarleton E.S. and Wakeman R.J., 2010, The porosity, permeability and restructuring of heterogeneous filter cakes, *Chemical Engineering & Technology*, **33**, 1-8. DOI: 10.1002/ceat.201000093